Web Guide Process in Cold Rolling Mill : Modeling and PID Controller

Byoung Joon Ahn
Department of Mechanical and Intelligent Systems Engineering, Pusan National University, JangJeon-Dong, KumJeung-Ku, Pusan 609-735, Korea
Ju Yong Choi
Department of Mechanical and Intelligent Systems Engineering, Pusan National University, JangJeon-Dong, KumJeung-Ku, Pusan 609-735, Korea
Yu Shin Chang
Department of Mechanical and Intelligent Systems Engineering, ERC/NSDM Pusan National University, JangJeon-Dong, KumJeung-Ku, Pusan 609-735, Korea
Man Hyung Lee*
School of Mechanical Engineering, Pusan National University, JangJeon-Dong, KumJeung-Ku, Pusan 609-735, Korea

There are many intermediate web guides in cold rolling mills process such as CRM (cold rolling mill), CGL (continuous galvanizing line), EGL (electrical galvanizing line) and so on. The main functions of the web guides are to adjust the center line of the web (strip) to the center line of the steel process. So they are called CPC (center position control). Rapid process speed cause large deviation between the center position of the strip and the process line. Too much deviation is not desirable. So the difference between the center position of the strip and the process line should be compensated. In general, the center position control of the web is obtained by the hydraulic driver and electrical controller. In this paper, we propose modelling and several controller designs for web-guide systems. We model the web and guide by using geometrical relations of the guide ignored the mass and stiffness of the web. To control the systems, we propose PID controllers with their gains tuned by the Ziegler-Nichols method, the H_∞ controller model-matching method, and the coefficient diagram method (CDM). CDM is modified for high order systems. The results are verified by computer simulations.

Key Words : Cold Rolling Mill, Center Position Control, PID, H_∞, CDM

1. Introduction

A continuous process system (Tahk and Shin, 2002) manufactures the web which is a flexible long strip such as steel, paper, printed textiles, and plastic products. Productivity in this process is related to the length and the speed of process. Increasing productivity causes a problem with the lateral movement and large camber of the web so that a device for compensating web position should be installed in the middle of the process. In particular, a wide web cannot be guided by means of flange and pulley because of undesirable distortion or damage of the edge.

In the steel industry, Markey (1957) researched the edge position control of webs. Feiertag (1967) studied steering and displacement type web guides in the rolling process. Guo et al (1999) imple-

* Corresponding Author,
E-mail : mahlee@pusan.ac.kr
TEL : +82-51-510-2331; **FAX** : +82-51-512-9835
School of Mechanical Engineering, Pusan National University, JangJeon-Dong, KumJeung-Ku, Pusan 609-735, Korea. (Manuscript **Received** June 16, 2003; **Revised** May 3, 2004)

mented center position control (CPC) in a cold mill with twin rolls by using two separated PID controllers. Shelton et al.(1971) had derived the first order and the second order model through geometrical relations taking into account the elasticity of webs, and represented dynamic behavior by regarding web as Euler beam. Using modified initial conditions, Young (1993) represented transfer function based on the second order model. System identification was used to control the web position by Besteman (1998). Campbell (1958) gave the responses of web position at a fixed roller for previous roller errors, which was the most simple web guide. Pivot steering-type web guide was analyzed by Sorsen (1966).

In spite of developing modern control theories, control loop has been constructed with a PID controller in various fields because of its simple structure, stable response to widespread processes, relatively efficient performance, and convenience for the operator. Up to now, much research of techniques to tune PID gains has been undertaken (1997), Ziegler and Nichols (1942). However in order to obtain further improvements in performance and stability against disturbances and parameter uncertainties, research of a synthetic tuning skills of gains is required. The coefficient diagram method (CDM) is one of gain-tuning techniques (Battacharyya et al., 1995 ; Manabe, 1998).

In this paper, the center position control of intermediate web guide will be performed by a PID controller, which is tuned to match up to the H_∞ controller. Furthermore, it is modified to be more robust for sinusoidal wave disturbances through a coefficient diagram and Lipatov lemma where the coefficient diagram reflects the stability, time responses, and robustness of a closed loop system ; and the Lipatov lemma provides the objective polynomial fitted on a design specification (Lipatov and Sokolov, 1979). Coefficients of a controller are represented in coefficient space and the controller has to be satisfied with linear inequality conditions. The norm is used for superior performance index.

Web and web-guide models are given in sec. 2. In sec. 3, a PID gain-tuning technique is discussed. Section 4 presents the simulation results of control with disturbances and parameter uncertainties. Finally, the discussion and main conclusions are given in sec. 5.

2. Process Modeling

2.1 Modeling of moving webs and web guides

in the cold rolling mill (Shin and Hong, 1998), it is difficult to derive a lateral dynamic equation of webs since it is affected by friction, tension, unknown physical properties of webs, and surface conditions of the contacting roller. Generally, a web entering onto any roller inclines to perpendicularly align to the roller. The curved web between nonparallel rollers is laterally vibrated because of the mass and stiffness of the web. So webs should be guided before rewinding through intermediate guides, which is accomplished by the shifting and swiveling of the rollers. Disregarding the mass and stiffness, a dynamic model of the web may be simply derived based on geometrical relations (Shelton and Reid, 1971). Under that assumption, the lateral velocity of web edge is proportional to the angle difference θ_r between nonparallel rollers and to the web longitudinal velocity V of the web. When the roller is moving laterally as z, the overall lateral velocity of web edge is represented by

$$\dot{y}_L = \dot{z} - V\theta_r \tag{1}$$

where y_L is the lateral displacement of web edge relative to the ground. Shelton (1971), Gere and Timoshenko (1993) derived the shape of the web by regarding the web as an Euler beam without mass, as follows :

$$\frac{\partial^4 y}{\partial x^4} - \frac{T}{EI}\frac{\partial^2 y}{\partial x^2} = 0 \tag{2}$$

where T is the total web tension and E is the modulus of elasticity (Young's modulus), and I is the lateral moment of inertia of the web.

There are two types of intermediate web guides : steering-type and displacement-type. In Fig. 1, the errors of web position can be reduced by steering the upstream roller which moves translationally and rotationally. Reflecting the

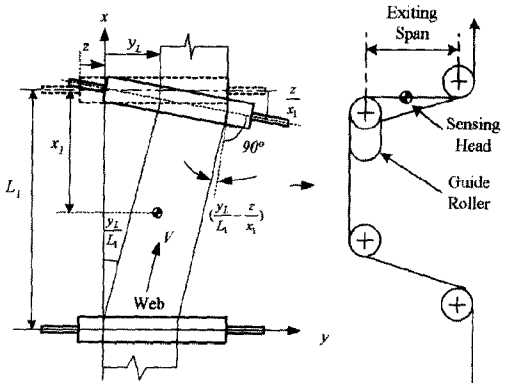

(a) Upside view (b) Side view

Fig. 1 Steering type web guide

rotation of the roller on the web model, the lateral velocity is obtained as

$$\dot{y}_L=\dot{z}+V\left(\frac{z}{x_1}-\frac{y_L}{L_1}\right) \tag{3}$$

where L_1 is the length of the entering span at the steering guide. Transfer function (with time constant $T_i=L_i/V$, i=1, 2, 3) from z to y_L is written as

$$\frac{Y_L(s)}{Z(s)}=\frac{T_1s+L_1/x_1}{T_1s+1} \tag{4}$$

Displacement type guide, as shown in Fig. 2, has two parallel upstream rollers. Through the lateral motion of the second upstream roller z, the first roller is laterally moved with velocity $(1-L_1/x_1)\dot{z}$. The lateral velocity of each roller is described as

$$\dot{y}_{L_3}=\left(1-\frac{L_1}{x_1}\right)\dot{z}-V\left(\frac{y_{L_3}}{L_3}\right) \tag{5}$$

$$\dot{y}_L=\dot{z}-V\left(\frac{y_L-y_{L_3}}{L_1}-\frac{z}{x_1}\right) \tag{6}$$

Through the above relations, the transfer function of displacement type guide can be derived.

$$\frac{Y_L(s)}{Z(s)}=\frac{T_3^2(L_1/L_3)s^2+T_3(1+L_1/L_3)s+L_1/x_1}{T_3^2(L_1/L_3)s^2+T_3(1+L_1/L_3)s+1} \tag{7}$$

In industrial application, the displacement of webs is measured in the middle of two parallel rollers due to the difficulty of installing sensors. If the exiting roller is assumed to be fixed as shown

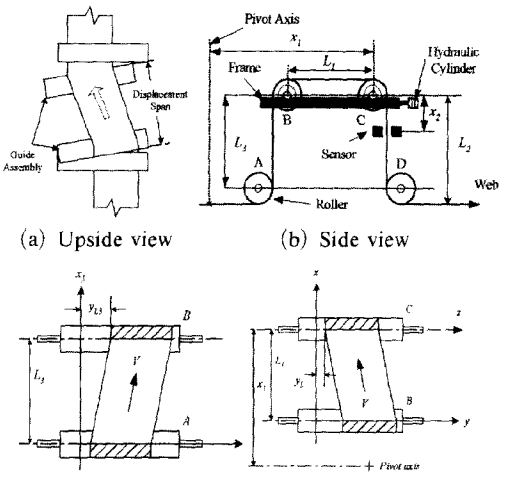

(a) Upside view (b) Side view

(c) Front view (d) Back side view

Fig. 2 Displacement type web guide

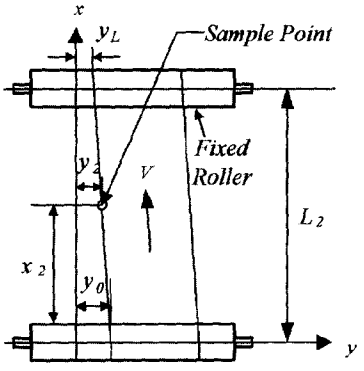

Fig. 3 Lateral displacement at a point between two parallel roller

in Fig. 3 and the web has a straight trajectory, the response y_2 is to be found at a sample point

$$\frac{Y_2(s)}{Y_0(s)}=\frac{T_2(1-x_2/L_2)s+1}{T_2s+1} \tag{8}$$

where x_2 is the distance from the entering roller to downstream.

2.2 Modeling of hydraulic driver

Hydraulic drivers are widely used to operate the guides in the steel industry. Figure 4 shows a hydraulic servo system which has many non-linear characteristics. Biased-load causes a velocity difference between going and returning. In this paper, the difference is regarded as disturbance

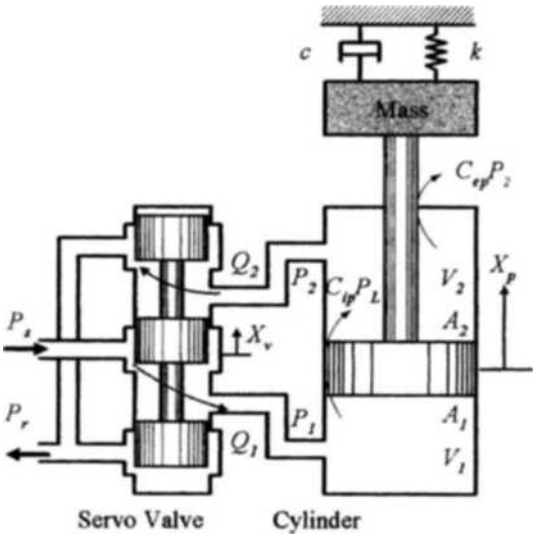

Fig. 4 Servo valve and cylinder

(Watton, 1989), servo valve is symmetric, supplied-pressure and falling-pressure at the valve orifice are constant, returned-pressure is zero, and there is no loss of friction at the pipe. Since applied current u stirs the spool in spite of the hysteresis of the torque motor, the servo valve is modeled as static represented by

$$x_v = K_{sv} u \tag{9}$$

Flow rate of the servo valve can be linearized at the operating point as

$$Q_L = k_1 x_v - k_2 P_L \tag{10}$$

where the coefficients are defined as follows

$$k_1 = \alpha C_d w_v \sqrt{\frac{1}{\rho}(P_s - P_{L0})}$$
$$k_2 = \frac{\alpha C_d w_v x_{v0}}{2\sqrt{(P_s - P_{L0})\rho}} \tag{11}$$

where C_d is the flow rate coefficient of orifice of the valve spool, w_w is the valve port gradient, ρ is hydraulic oil density, P_s is supplied-pressure, P_L is load-pressure. Disregarding leakage and compression of oil, cylinder flow rate is obtained as

$$Q_L = A_m \dot{x}_p \tag{12}$$

where A_m is the average area of the piston. The dynamic equation of the piston for external force F_L is described as

$$m\ddot{x}_p + c\dot{x}_p + kx_p + F_L = F$$
$$F = A_1 P_1 - A_2 P_2 \tag{13}$$

Therefore, the second order hydraulic driver is represented by

$$X_p(s) = \frac{A_e \frac{k_1}{k_2} x_v(s) - F_e(s)}{ms^2 + \left(c + \frac{A_e A_m}{K_t}\right)s + k} \tag{14}$$

where A_e is equivalent of the piston area, F_e is equivalent the external force, and K_t is the total pressure coefficient.

3. PID Controller of Web Guide

For a long time, most systems have adopted a PID controller because of its simplicity and intuitive gain tuning. There are many tuning techniques such as the Ziegle-Nichols method, the Kappa-Tau method, pole placement, and so on (Levine, 1996). In this paper, PID gains are tuned by a model matching the H_∞ controller and the coefficient diagram method (CDM).

3.1 Model matching method

It is well known that H_∞ control offers analytic and numerically stable solutions. However, the technique proposed by Doyle et al.(1989) cannot be applied to systems with invariant zeros on the infinite real axis or the imaginary axis and does not have an explicit relationship among free parameter, controller, and closed-loop characteristic equation. Owing to the high order of a controller, controller reduction is also needed to implement it. For alternative plan of these limitations, Gahinet (1994 ; 1996) presented H_∞ control based on bounded real lemma. Constraint equation is described by linear matrix inequality (LMI) including a reduced order controller.

If PID gains are tuned to match up with a H_∞ controller, it is both robust and simple. Model matching is accomplished by comparing the H_∞ controller with loop transfer functions including a PID controller in the frequency domain. Generally a PID controller with k_p, k_i and k_d is written as

$$K_P(s)=k_p+\frac{k_i}{s}+k_d s \tag{15}$$

The loop transfer function of a H_∞ controller is $L_H(s)=G(s)K_P(s)$. $L_H(j\omega)$, $G(j\omega)$, and $K_P(j\omega)$ are the frequency responses of $L_H(s)$, $G(s)$, and $K_P(s)$, and can be described as

$$\begin{aligned} G(j\omega)&=G_r(\omega)+jG_i(\omega)\\ L_H(j\omega)&=L_{Hr}(\omega)+jL_{Hi}\\ K_P(j\omega)&=K_{Pr}(\omega)+jK_{Pi}(\omega) \end{aligned} \tag{16}$$

where $K_{Pr}(\omega)=k_p$, $K_{Pi}(\omega)=k_d\omega-k_i/\omega$. Error equation is defined as follows

$$E(j\omega)=L_H(j\omega)-G(j\omega)K_P(j\omega) \tag{17}$$

By applying errors $E(j\omega_i)$ for $\omega_i\in[\omega_{\min}\ \omega_{\max}]$ (i=1, 2, ···, N), where $\omega_{\max}$ is a little larger than cut-off frequency (Gahinet and Apkarian, 1994), cost function J is obtained as

$$\begin{aligned} J&=\sum_{i=1}^{N}|E(j\omega_i)^2|\\ &=\sum_{i=1}^{N}|L_H(j\omega_i)-G(j\omega_i)K_P(j\omega_i)|^2 \end{aligned} \tag{18}$$

Separating real and imaginary parts, $E(j\omega)$ is described as

$$\begin{bmatrix} E_r(\omega)\\ E_i(\omega)\end{bmatrix}=\begin{bmatrix} L_{Hr}(\omega)\\ L_{Hi}(\omega)\end{bmatrix}-\Phi(\omega)\begin{bmatrix} k_p\\ k_i\\ k_d\end{bmatrix} \tag{19}$$

where $\Phi(\omega)$ is given by

$$\Phi(\omega)=\begin{bmatrix} G_r(\omega) & G_i(\omega)\frac{1}{\omega} & -G_i(\omega)\omega\\ G_i(\omega) & -G_r(\omega)\frac{1}{\omega} & G_r(\omega)\omega\end{bmatrix} \tag{20}$$

From eq. (19), eq (18) is developed as

$$\begin{aligned} J&=\sum_{i=1}^{N}[E_r(\omega_i)^2+E_i(\omega_i)^2]\\ &=(\beta-\Lambda\alpha)^T(\beta-\Lambda\alpha) \end{aligned} \tag{21}$$

where matrices Λ, α, and β are defined as follows

$$\begin{aligned} \Lambda&=[\Phi(\omega_1)\ \Phi(\omega_2)\ \cdots\ \Phi(\omega_N)]\\ \beta&=[L_{Hr}(\omega_1)\ L_{Hi}(\omega_1)\ \cdots\ L_{Hr}(\omega_N)\ L_H(\omega_N)]\\ \alpha&=[k_p\ k_i\ k_d]^T \end{aligned} \tag{22}$$

PID gains to minimize J are calculated by the least mean square (pseudo-inverse) method (Gilbert Strang, 1986) as

$$\alpha=(\Lambda^T\Lambda)^{-1}\Lambda^T\beta \tag{23}$$

3.2 Coefficient diagram method (CDM)

Modern control theories provide robustness and optimality but have difficulties in selecting weight functions. CDM designs a simple controller based on pole placement for a characteristic equation whose coefficients are represented by stability index γ_i and equivalent time constant τ. This method can be applied to single-input/single-output systems and corresponds with specifications in time domain (Manabe, 1998). In a coefficient plot as semi-log diagram, convexity, slop, and shape, the plot are related to stability, response speed, and robustness. If the characteristic equation cannot be determined to fit the given constraint and fundamental specification, the structure of the controller should be modified. Figure 5 shows the standard block diagram for CDM where characteristic equation is represented by

$$\begin{aligned} P(s)&=A(s)D(s)+B(s)N(s)\\ &=a_n s^n+a_{n-1}s^{n-1}+\cdots+a_1 s+a_0 \end{aligned} \tag{24}$$

In (Manabe, 1998), stability index γ_i, stability limit γ_i^*, and equivalent time constant τ are defined as follows

$$\gamma_i=\frac{a_i^2}{a_{i+1}a_{i-1}}\quad(i=1,\ n-1) \tag{25}$$

$$\gamma_i^*=\frac{1}{\gamma_{i+1}}+\frac{1}{\gamma_{i-1}}\quad(\gamma=\gamma_0=\infty) \tag{26}$$

$$\tau=\frac{a_i}{a_0} \tag{27}$$

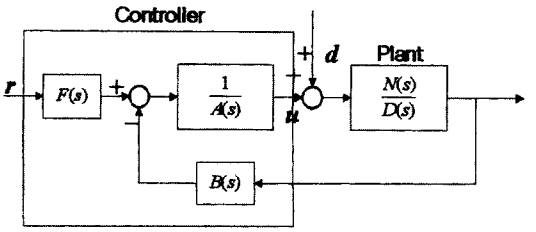

Fig. 5 CDM standard block diagram

Then, characteristic equation and each coefficient is obtained as stability index and equivalent time constant, as follows

$$P(s)=a_0\left[\left\{\sum_{i=2}^{n}\left(\prod_{j=1}^{i-1}\frac{1}{\Gamma_j}\right)(\tau\cdot s)^i\right\}+(\tau\cdot s)+1\right] \quad (28)$$

$$a_i=a_0\tau^i/\gamma_{i-2}^2\cdots\gamma_2^{i-2}\gamma_1^{i-1} \quad (29)$$

In order to design a controller by CDM, the equivalent time constant τ should be selected firstly to be 2.5~4 times of settling time. Manabe (1998) recommended the stability indexes as $\gamma_0=\gamma_1=\gamma_2=2$, $\gamma_3=2.5$ and $\gamma_i>1.5\gamma_i^*$ (for $i=4, 5, \cdots, n-1$). Substituting τ and γ_i to Eq. (29), coefficients of the characteristic equation can be calculated. For the fifth order system with $\tau=5$, the coefficient diagram is as shown in Fig. 6, and the characteristic equation is written as

$$P(s)=0.25s^5+s^4+2s^3+2s^2+s+0.2 \quad (30)$$

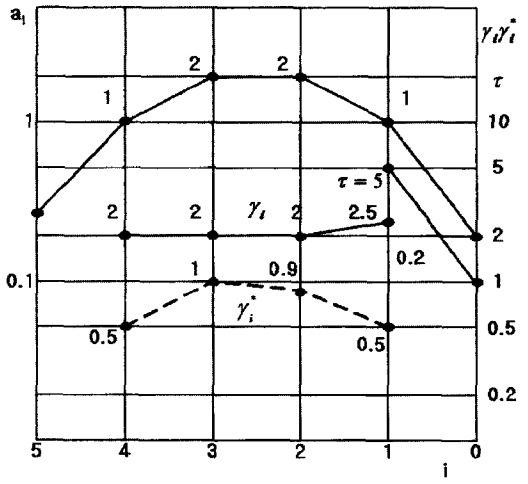

Fig. 6 Coefficient diagram for the fifth order system

Figure 7 shows the effects of γ_i and τ in the coefficient diagram. The larger γ_i and τ are, the higher diagrams are, where stability is the counterpart of response speed. Therefore, a convex diagram guarantees stability and robustness.

The fixed values γ_i are normally used by Butterworth and ITAE prototypes (Battacharyya et al., 1995), although τ and γ_i can be arbitrarily set up by the designer. For systems having uncertainties, stability is assured by using the Kharitonov theorem and Lipatov theorem (Lipatov and Sokolov, 1979), where the robustness index γ_i^{**} with $a_i\in[a_i^{\min}, a_i^{\max}]$ $(i=1, \cdots, n-1)$ are defined as follows

$$\gamma_i^{**}=\min\left\{\frac{(a_i^{\min})^2}{a_{i+1}^{\min}a_{i-1}^{\max}}, \frac{(a_i^{\min})^2}{a_{i-1}^{\max}a_{i+1}^{\min}}\right\}, \ (i=1, \cdots, n-1) \quad (31)$$

Then, the characteristic equation is Hurwitz stable (Battacharyya et al., 1995) if γ_i^{**} $(i=1, \cdots, n-1)$ are satisfied with

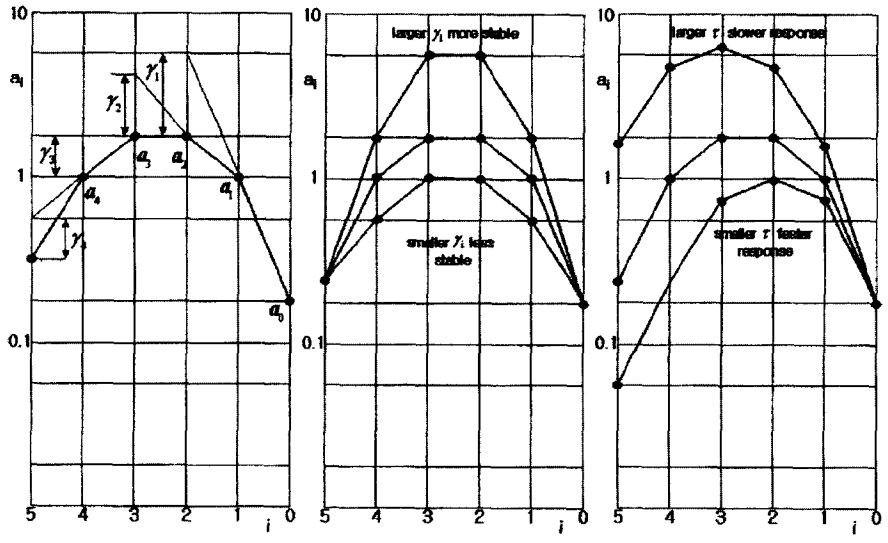

(a) Incremental ratio for γ_i (b) Stability (c) Responsibility

Fig. 7 Design procedure by using coefficient diagram

$$\sqrt{\gamma_{i-1}^{**}\gamma_i^{**}}>1.4656 \tag{32}$$

where the value is induced by Manabe Standard type (Manabe, 1998).

The linear constraint equation (Young and Reid, 1993) should be satisfied since the characteristic equation is represented as a linear function for the given controller coefficient.

$$\delta_i^{T-}\leq\delta_i(X,\ P_v)\leq\delta_i^{T+} \tag{33}$$

where X is the coefficient space of the controller and P_v is the maximum and minimum value of each coefficient. When the controller is selected in X, the system is stable and accords with the given specifications. In addition, robustness is improved by increasing l_2 stability margin that Keel (1999) introduced for analysis of the closed-loop stability for variation of controller coefficients. Coefficient sets which satisfy the linear constraint conditions have to be divided with a proper interval owing to nonlinearity of l_2 stability margin.

3.3 PID controller by CDM

Manabe criterion cannot be applied to the fourth or larger order systems. Therefore, this paper modifies the PID controller based on CDM for the center position control of intermediate web guide. If the CDM standard block diagram in Fig. 5 is defined as follows,

$$\begin{aligned}A(s)&=l_2s^2+l_1s+l_0\\B(s)&=K_2s^2+K_1s+K_0\\F(s)&=m_2s^2+m_1s+m_0\end{aligned} \tag{34}$$

then the coefficients of PID controller are represented as

$$\begin{aligned}m_2&=K_2=K_d\\m_1&=K_1=K_p\\m_0&=K_0=K_i\\l_2&=l_0=0,\text{ and }l_1=1\end{aligned} \tag{35}$$

However, the parameter l_2 should be assigned to small value T_d for the purpose of increasing response speed. Manabe determined T_d=0.05, whereas this paper determined T_d=0.01 by trial and error method. Figure 8(a) shows the results

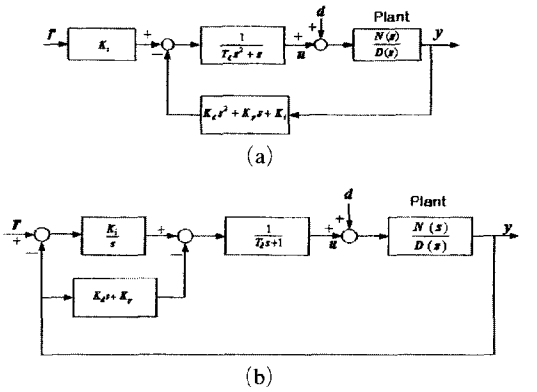

(a) (b)

Fig. 8 Modified PID Controller by CDM

of a modified PID controller. Hence, the PID controller is converted to the I-PD controller. Moreover, PID gains maximizing the l_2 stability margin are selected to improve robustness. For the system parameter vector P, and its nominal vector P^0, the characteristic equation is written as

$$\delta(s,\ P)=\delta_0(P)+\delta_1(P)s+\delta_2(P)s^2+\cdots \tag{36}$$

If $\delta(s,\ P^0)$ is stable for the intriguing stable region S, perturbation of the parameter is given by

$$\begin{aligned}\Delta P&=P-P^0\\&=[P_1-P_1^0,\ P_2-P_2^0,\ \cdots,\ P_l-P_l^0]\end{aligned} \tag{37}$$

Using the parametric norm, the open-ball with radius ρ is defined as follows

$$B(\rho,\ P^0)=\{P:\|P-P^0\|<\rho\} \tag{38}$$

A polynomial group concerning $B(\rho,\ P^0)$ is obtained as

$$\Delta\rho(s)=\{\delta(s,\ P^0+\Delta P)\,|\,\|\Delta P\|<\rho\} \tag{39}$$

When the largest radius nearby P^0 is defined as $\rho^*(P^0)$, the stability margin is written by $P\in B(\rho^*(P^0),\ P^0)$ in the coefficient space. That is, this margin guarantees perturbation range. An arbitrary point $s^*\in\partial S$ to be the solution of $\delta(s,\ P^0+\Delta P)$ satisfies the following equations,

$$\delta(s^*,\ P^0)+a_1(s^*)\Delta P_1+\cdots+a_l(s^*)\Delta P_l=0 \tag{40}$$

where a_{in} is the coefficient of the n-th order of

$a_i(s)$. The real and imaginary parts of the above equation are represented by

$$A(s_r)\ T(s_r)=b(s_r)$$
$$[a_r(s_r)\ \cdots\ a_l(s_r)]\begin{bmatrix}\triangle P_1\\ \vdots\\ \triangle P_l\end{bmatrix}=-\delta^0(s_r) \tag{41}$$

$$A(s_c)\ T(s_c)=b(s_c)$$
$$\begin{bmatrix}a_{1r}(s_c) & \cdots & a_{lr}(s_c)\\ a_{1i}(s_c) & \cdots & a_{li}(s_c)\end{bmatrix}\begin{bmatrix}\triangle P_1\\ \vdots\\ \triangle P_l\end{bmatrix}=\begin{bmatrix}-\delta_r^0(s_c)\\ -\delta_i^0(s_c)\end{bmatrix} \tag{42}$$

where s_r is a real number and s_c is a complex number. The l_2 stability margin is obtained as

$$\rho^*=\min\{\|t^*(s_c)\|_2,\ \|t^*(s_r)\|_2\} \tag{43}$$

$$t^*(s_c)=A^T(s_c)[A(s_c)A^T(s_c)]^{-1}b(s_c) \tag{44}$$

$$t^*(s_r)=A^T(s_r)[A(s_r)A^T(s_r)]^{-1}b(s_r) \tag{45}$$

$$t_n^*=A_n^T[A_nA_n^T]^{-1}b_n \tag{46}$$

When the rank of $A(s_c)$ is equal to zero, the radius $\rho(s_c)$ of open-ball diverges to infinity. If Rank$[A(s_c)]=1$, the rank of $[A(s_c),\ b(s_c)]$ should be 1 in order to converge; otherwise the radius diverges too. The coefficients of the controller are selected when the l_2 stability margin is maximized for each coefficient partition satisfying the linear constraint.

4. Simulation Results

The robustness against disturbance and parameter uncertainties at the center position systems is verified here by computer simulation. The systems are controlled by the PID controller differently tuned by the Ziegler-Nichols method, H_∞ model-match method, and coefficient diagram method. Model uncertainties exist in the web speed $V\in[1, 5]$m/s and load pressure $P_L\in[20, 200]$kgf/cm^2, where the nominal values are $V_0=3$ m/s and $P_{L0}=60$ kgf/cm^2. Then the transfer functions of the steer type and the displacement type guides are represented by

$$G_s(s)=\frac{\beta_{S2}s^2+\beta_{S1}s+\beta_{S0}}{s^4+\alpha_{S3}s^3+\alpha_{S2}s^2+\alpha_{S1}s+\alpha_{S0}} \tag{47}$$

$$G_D(s)=\frac{\beta_{D3}s^3+\beta_{D2}s^2+\beta_{D1}s+\beta_{D0}}{s^5+\alpha_{D4}s^4+\alpha_{D3}s^3+\alpha_{D2}s^2+\alpha_{D1}s+\alpha_{D0}} \tag{48}$$

where the coefficients of steering type are $\beta_{S2}\in[4.2, 21]$, $\beta_{S1}\in[3, 16]$, $\beta_{S0}\in[0.5, 2.6]$, $\alpha_{S3}\in[3, 8]$, $\alpha_{S2}\in[1, 2.5]$, $\alpha_{S1}\in[0.05, 0.15]$, and $\alpha_{S0}\in[0, 0]$; and the coefficients of displacement type are $\beta_{D3}\in[4.5, 24]$, $\beta_{D2}\in[5, 29]$, $\beta_{D1}\in[0.9, 5]$, $\beta_{D0}\in[0.05, 0.3]$, $\alpha_{D4}\in[4.9]$, $\alpha_{D3}\in[4, 9]$, $\alpha_{D2}\in[0.7, 2]$, $\alpha_{D1}\in[0.03, 0.08]$, and $\alpha_{D0}\in[0, 0]$. In the cold rolling mill, lateral disturbance is a sinusoidal wave with 120 mm amplitude and 2 rad/s frequency when the speed and the width of web are 5 m/s and 1000 mm.

Figure 9 shows the coefficient diagrams for the

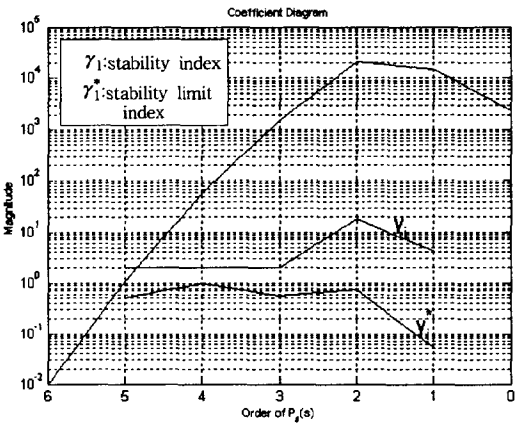

(a) Steering type web guide

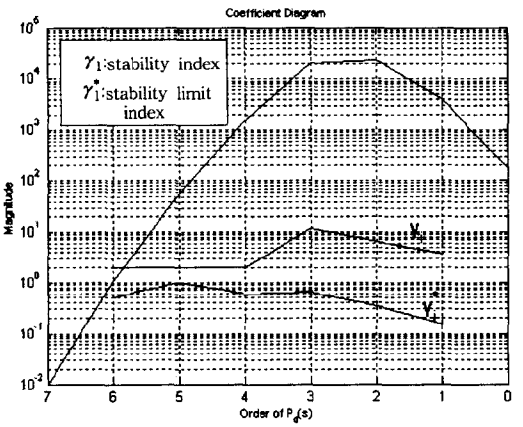

(b) Displacement type web guide

Fig. 9 Coefficient diagrams of each web guide

steering-type and the displacement-type web-guide systems where the stability indexes and stability limits are obtained as

$$\gamma_{Si}=[4.36,\ 18.6,\ 2,\ 2,\ 2] \qquad (49)$$
$$\gamma^*_{Si}=[0.05,\ 0.73,\ 0.55,\ 1,\ 0.5]$$

$$\gamma_{Di}=[3.74,\ 6.65,\ 12.07,\ 2,\ 2,\ 2] \qquad (50)$$
$$\gamma^*_{Di}=[0.15,\ 0.35,\ 0.65,\ 0.58,\ 1,\ 0.5]$$

Because these indexes and limits fit the stability conditions, the PID controller is appropriately tuned by CDM.

Figures 10-12 show the results for the steering type web guide. As shown in Fig. 10, the PID controller by CDM has the best sensitivity performance at low frequencies and has good regu-

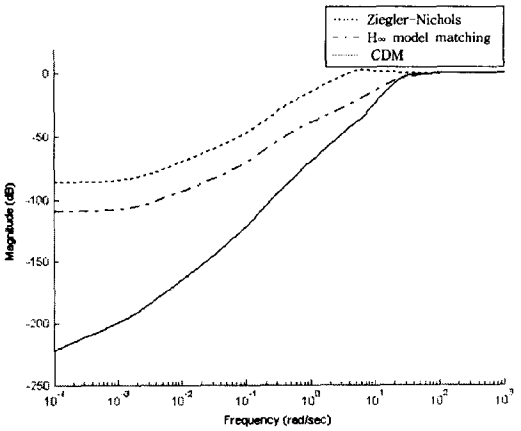

(a) Sensitivity functions

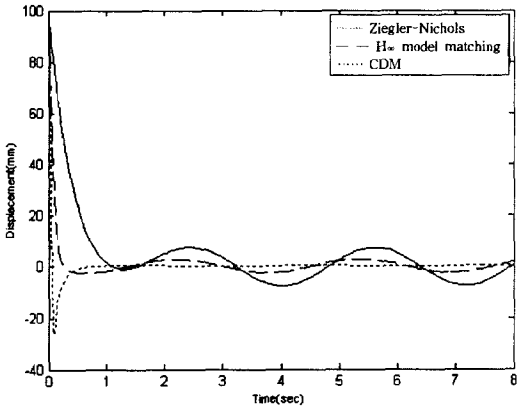

(b) Responses for disturbance

Fig. 10 Response of the steering type for the disturbance

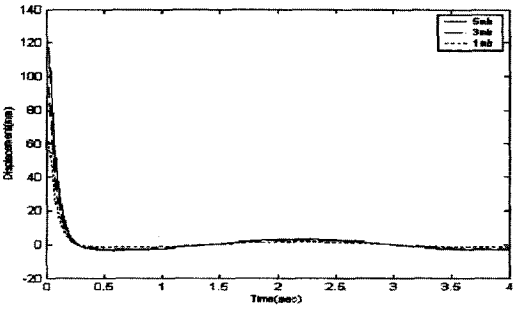

(a) PID controller by H_∞ model matching

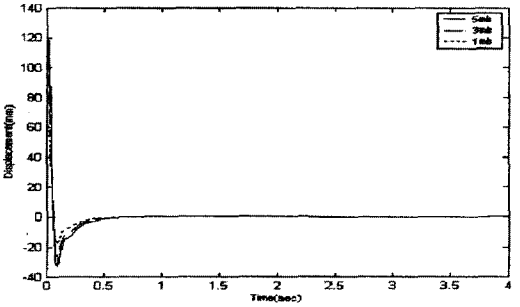

(b) PID controller by CDM

Fig. 11 Responses of the steering type for the speed variation

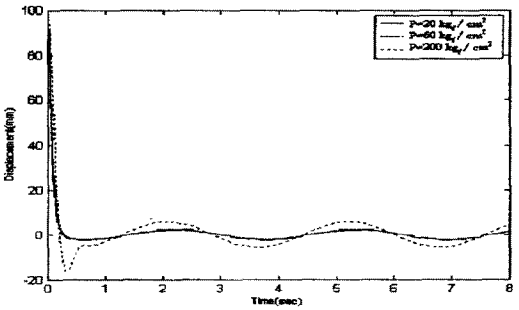

(a) PID controller by H_∞ model matching

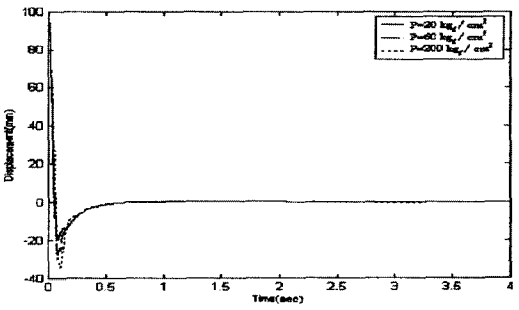

(b) PID controller by CDM

Fig. 12 Responses of the steering type for the load pressure variation

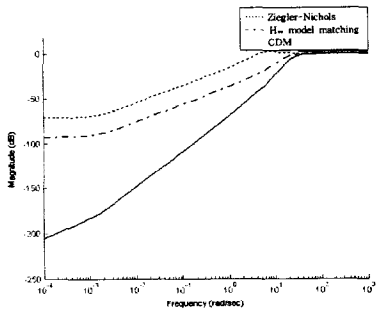

(a) Sensitivity functions

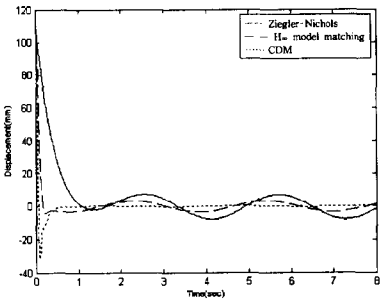

(b) Responses for disturbance

Fig. 13 Responses of the displacement type for the disturbance

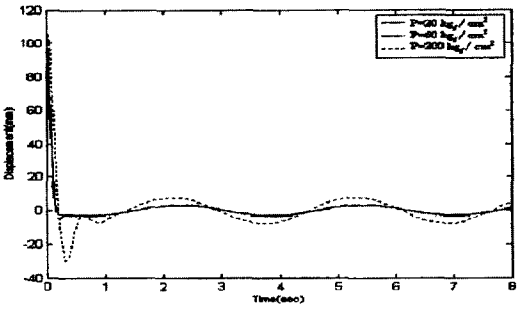

(a) PID controller by H_∞ model matching

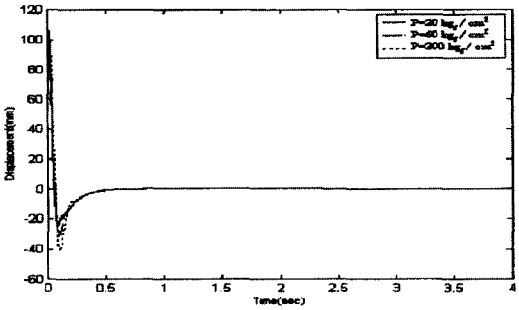

(b) PID controller by CDM

Fig. 15 Responses of the displacement type for the load pressure variation

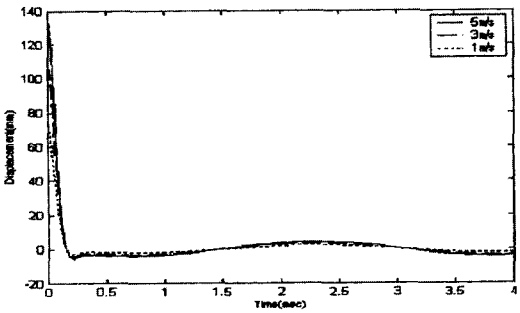

(a) PID controller by H_∞ model matching

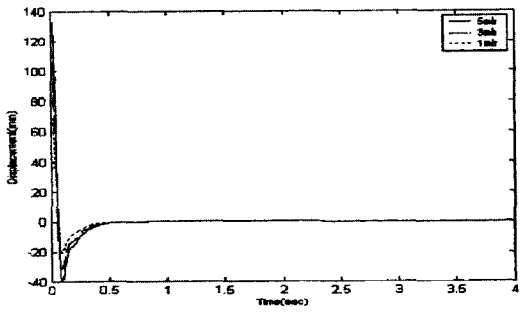

(b) PID controller by CDM

Fig. 14 Responses of the displacement type for the speed variation

lation performance for sinusoidal disturbance. Actually the variation of web speed affects the amplitude of the sinusoidal disturbance, i.e. the speed-up of web enlarges the disturbance amplitude. Figure 11 shows the regulation responses of each controller for the variation of web speed, where the CDM is the most robust. Moreover, the initial undershoot is of no importance in a web-guide system because there is just a small part as opposed to a long strip being removed. For variation of load pressure, Fig. 12 shows the response by the model-match and the CDM. In spite of initial undershoot, CDM is more robust also. The displacement type shows similar results in Fig. 13-15 Therefore CDM is apt for the web guide system because the controllers via CDM have higher control-gains than others under the same design specification.

5. Conclusion

This paper dealt with intermediate web guides in a cold rolling mill. To locate the web on the

center position of roller, a PID controller was used. The web and guides were modeled as the second-order system for the steering type and the displacement type by using geometrical relations ignoring the mass and stiffness of the web. The hydraulic driver as the actuator laterally moving the roller was modeled simply here. A PID controller for the center position control was tuned by the Ziegler-Nichols method, the H_∞ controller model-matching method, and coefficient diagram method(CDM). For CDM, the basic PID controller was modified and l_2 norm was used to improve robustness. For sinusoidal disturbance at the roller and load pressure variation at the hydraulic driver, controllers were verified by computer simulation, where the CDM proved to be the most robust against disturbance and parameter variation.

Acknowledgment

This research was financially supported by Korea Science and Engineering Foundation (KOSEF) through the Engineering Research Center for Net Shape and Die Manufacturing (ERC/NSDM) at Pusan National University and by Pusan National University Research Grant.

References

Battacharyya, S. P., Keel, L. H. and Ikeda, M., 1995, *Robust Control : The Parametric approach*, Prentice-Hall.

Besteman, M. P. G. J., Limpens, C. H. L., Babuska, R., Otten, J. B. and Verhaegen, M., 1998, "Modeling and Identification of a Strip Guidance Process with Internal Feedback," *IEEE Transactions on Control Systems and Technology*, Vol. 6, No. 1, pp. 88~102.

Campbell, D. P., 1958, *Process Dynamics*, Wiley, New York, pp. 152~156.

Doyle, J. C., Glover, K., Khargonekar, P. P. and Francis, B. A., 1989, "State-Space Solutions to Standard H_2 and H_∞ Control Problems," *IEEE Transactions on Automatic Control*, Vol. 34, No. 8, pp. 831~847.

Feiertag, B. A., 1967, "Intermediate Guiding On Steel Strip Processing Lines," *Iron and Steel Engineer*, pp. 147~155.

Gahinet, P. and Apkarian, P., 1994, "A Linear Matrix Inequality Approach to H_∞ Control," *International Journal of Robust and Nonlinear Control*, Vol. 4, pp. 421~448.

Gahinet, P., 1996, "Explicit Controller Formulas for LMI-based H_∞ Synthesis," *Automatica*, Vol. 32, No. 7, pp. 1007~1014.

Gere, J. M. and Timoshenko, 1993, *Mechanics of Material, Third Edition*, Thomson Publishing.

Gilbert Strang, 1986, *Linear Algebra and Its Applications*, 3rd edition, Harcourt Brace Jovanovich.

Guo, R. M. and Loen, M. V., 1999, "Design and Simulation of an Entry Edge Guide Control System for Tandem Cold Mills," *Journal of Manufacturing Science and Engineering*, Vol. 121, pp. 69~75.

Keel, L. H. and Battacharyya, S. P., 1999, "Robust Stability and Performance with Fixed-Order Controller," *Automatica*, Vol. 35, pp. 1717~1724.

Kyung-Mo Tahk and Kee-Hysn Shin, 2002, "A Study on the Fault Diagnosis of Roller-Shape Using Frequency Analysis of Tension Signals and Artificial Neural Networks Based Approach in a Web Transport System," *KSME International Journal*, Vol. 16, No. 12, pp. 1604~1612, in Korea.

Levine, 1996, *The Control Handbook*, CRC Press, Vol. 2, pp. 819~823.

Lipatov, A. V. and Sokolov, N. I., 1979, "Some Sufficient Condition for Stability and Instability of Continuous Linear Stationary Systems," *Automatic Remote Control*, No. 39, pp. 1285~1291.

Manabe, S., 1998, "Coefficient Diagram Method," *14th IFAC Symposium on Automatic Control in Aerospace*, pp. 199~210.

Markey, F. J., 1957, "Edge Position Control for the Steel Strip Industry," *Iron and Steel Engineer*, pp. 119~131.

Ogata, K., 1997, *Modern Control Engineering*, Pretice-Hall.

Shelton, J. J. and Reid, K. N., 1971, "Lateral Dynamics of an Idealized Moving Web," *Journal of Dynamic Systems, Measurement, and Control*,

pp. 187~192.

Shin, K. H. and Hong, W. K., 1998, "Real-Time Tension Control in a Multi-Stand Rolling System," *KSME International Journal*, Vol. 12, No. 1, pp. 12~21, in Korea.

Sorsen, S. L., 1966, "Controlling Web Position," *Automatica*, pp. 105~110.

Watton, J., 1989, *Fluid Power Systems*, Prentice-Hall.

Young, G. E. and Reid, K. N., 1993, "Lateral and Longitudinal Dynamic Behavior and Control of Moving Webs," *Journal of Dynamic Systems, Measurement, and Control*, pp. 309~317.

Ziegler, J. G. and Nichols, N. B., 1942, "Optimum Settings for Automatic Controllers," *Transactions of ASME*, Vol. 64, pp. 759~768.

Shelton, J. J. and Reid, K. N., 1971, "Lateral Dynamics of an Real Moving Web," *Journal of Dynamic Systems, Measurement, and Control*, pp. 180~186.